Murine models of acute neuronopathic Gaucher disease

Ida Berglin Enquist*, Christophe Lo Bianco†, Andreas Ooka*, Eva Nilsson*, Jan-Eric Månsson‡, Mats Ehinger§, Johan Richter*, Roscoe O. Brady¶‖, Deniz Kirik**, and Stefan Karlsson*‖

*Molecular Medicine and Gene Therapy, Institute of Laboratory Medicine and the Strategic Research Center for Stem Cell Biology and Cell Therapy, Lund University, BMC A12, 221 84 Lund, Sweden; †Division of Neurobiology and **CNS Disease Modeling Unit, Department of Experimental Medical Science, Wallenberg Neuroscience Center, Lund University, BMC A11, 221 84 Lund, Sweden; ‡Institute of Clinical Neuroscience, Sahlgrenska University Hospital, 431 80 Mölndal, Sweden; §Department of Pathology, Lund University Hospital, 221 00 Lund, Sweden; and ¶Developmental and Metabolic Neurology Branch, National Institute of Neurological Disorders and Stroke, National Institutes of Health, Bethesda, MD 20892-1260

Contributed by Roscoe O. Brady, August 31, 2007 (sent for review August 1, 2007)

Gaucher disease (GD) is an autosomal recessive lysosomal storage disorder caused by mutations in the glucosidase, beta, acid (GBA) gene that encodes the lysosomal enzyme glucosylceramidase (GCase). GCase deficiency leads to characteristic visceral pathology and, in some patients, lethal neurological manifestations. Here, we report the generation of mouse models with the severe neuronopathic form of GD. To circumvent the lethal skin phenotype observed in several of the previous GCase-deficient animals, we genetically engineered a mouse model with strong reduction in GCase activity in all tissues except the skin. These mice exhibit rapid motor dysfunction associated with severe neurodegeneration and apoptotic cell death within the brain, reminiscent of neuronopathic GD. In addition, we have created a second mouse model, in which GCase deficiency is restricted to neural and glial cell progenitors and progeny. These mice develop similar pathology as the first mouse model, but with a delayed onset and slower disease progression, which indicates that GCase deficiency within microglial cells that are of hematopoietic origin is not the primary determinant of the CNS pathology. These findings also demonstrate that normal microglial cells cannot rescue this neurodegenerative disease. These mouse models have significant implications for the development of therapy for patients with neuronopathic GD.

lysosomal storage disorder | glucocerebrosidase deficiency | neurodegeneration | knockout mice | gene therapy

Gaucher disease (GD) is the most prevalent lysosomal storage disorder. Inherited deficiency of glucosylceramidase (GCase) causes storage of glucosylceramide (glccer), mainly in the macrophages throughout the body, with consequent hepatosplenomegaly, cytopenias, and bone disease as key clinical features (1, 2). Patients with the disorder are commonly subdivided into three clinical phenotypes based on the absence (type 1) or presence and severity (types 2 and 3) of central nervous system (CNS) involvement (2). Enzyme replacement therapy is highly effective in treating the visceral manifestations of GD (3–6). However, intravenously administered GCase cannot cross the blood–brain barrier and is therefore unable to alleviate the CNS involvement in neuronopathic GD (7).

Infantile (Type 2) neuronopathic GD is characterized by early onset, rapid progression, extensive CNS pathology, and death, usually by 2 years of age (2, 8, 9). Frequent pathological findings in these patients are neurodegeneration, astrogliosis, microglial proliferation, and increased levels of glccer and glucosylsphingosine in the brainstem, cerebellum, hippocampus, basal ganglia, thalamus, and cortex (2, 10–16). Common neurological signs include hypertonia of the neck, apnea, feeding difficulties, and seizures (8, 9). The first GCase-deficient mouse was created by insertion of the neomycin resistance gene into glucosidase, beta, acid (gba) exons 9 and 10 (17). These mice died very soon after birth primarily because of excessive water loss through the skin (18). We and others have created viable mouse models of type 1 (nonneuronopathic) GD (19, 20), but there has been no GCase-deficient mouse that displays the severe CNS manifestations of neuronopathic GD that survived more than a few hours. Here, we describe the creation of mouse models with features closely simulating severe neuronopathic GD. Our findings have important implications, not only toward increased knowledge of the relationship between GCase deficiency and the neurological manifestations of type 2 GD, but also with regard to the mandatory target cells for the therapy for severe neuronopathic GD.

Results

Retention of a Marker Cassette in gba Intron 8 Causes Perturbed Splicing and Reduced GCase Activity Levels. To disrupt GCase activity, we inserted a loxp-neo-loxp (lnl) cassette into intron 8 of the murine gba gene (Fig. 1*A*). Homozygous lnl ($gba^{lnl/lnl}$) mice died within hours after birth with a similar skin phenotype to that observed in the first GCase-deficient mouse (17, 18) (Fig. 1*B*). To restore normal epidermal function while maintaining GCase deficiency in all other tissues including the brain, $gba^{lnl/lnl}$ mice were bred with K14-Cre transgenic mice (21), in which cre recombinase expression is driven by the K14 promoter allowing recombination of $gba^{lnl/lnl}$ within the skin (Fig. 1 *A* and *C*). The gba^{lnl} allele produced very low levels of gba mRNA, at least in part because of abnormal splicing of gba mRNA [Fig. 1*D* and supporting information (SI) Fig. 5]. Correctly spliced gba mRNA was also present at low levels in these mice (hereafter referred to as K14-lnl/lnl mice), which explained the residual GCase activity in the K14-lnl/lnl tissues (Fig. 1 *D* and *E* and SI Fig. 5). The K14-lnl/lnl mice had abnormal levels of Glccer in brain, spleen, and liver (Fig. 1*F*). Analysis of the molecular species of the glccer in the K14-lnl/lnl brains showed that Glccer with C18 fatty acid constituted >80% (data not shown). This finding is in agreement with earlier reports on GD type 2 patients (22). Furthermore, visceral Gaucher cells, which are highly characteristic of all types of GD (2), were present in spleen and liver of K14-lnl/lnl mice (SI Fig. 6)

K14-lnl/lnl Mice Display a Severe and Rapidly Progressive Neurological Disease Associated with Neuron Loss and Massive Microglia Activation and Proliferation. In contrast to previously developed GCase-deficient mice, which have either been perinatally lethal or

Author contributions: I.B.E. and C.L.B. contributed equally to this work; I.B.E., C.L.B., A.O., and S.K. designed research; I.B.E., C.L.B., A.O., E.N., J.-E.M., and M.E. performed research; I.B.E., C.L.B., E.N., D.K., and S.K. analyzed data; and I.B.E., C.L.B., J.R., R.O.B., and S.K. wrote the paper.

The authors declare no conflict of interest.

Abbreviations: GCase, glucosylceramidase EC 3.2.1.21 (acid β-glucosidase); GD, Gaucher disease; Glccer, glucosylceramide; GBA, glucosidase, acid, beta; lnl, loxP-neo-loxP.

‖To whom correspondence may be addressed. E-mail: rb57v@nih.gov or stefan.karlsson@med.lu.se.

This article contains supporting information online at www.pnas.org/cgi/content/full/0708086104/DC1.

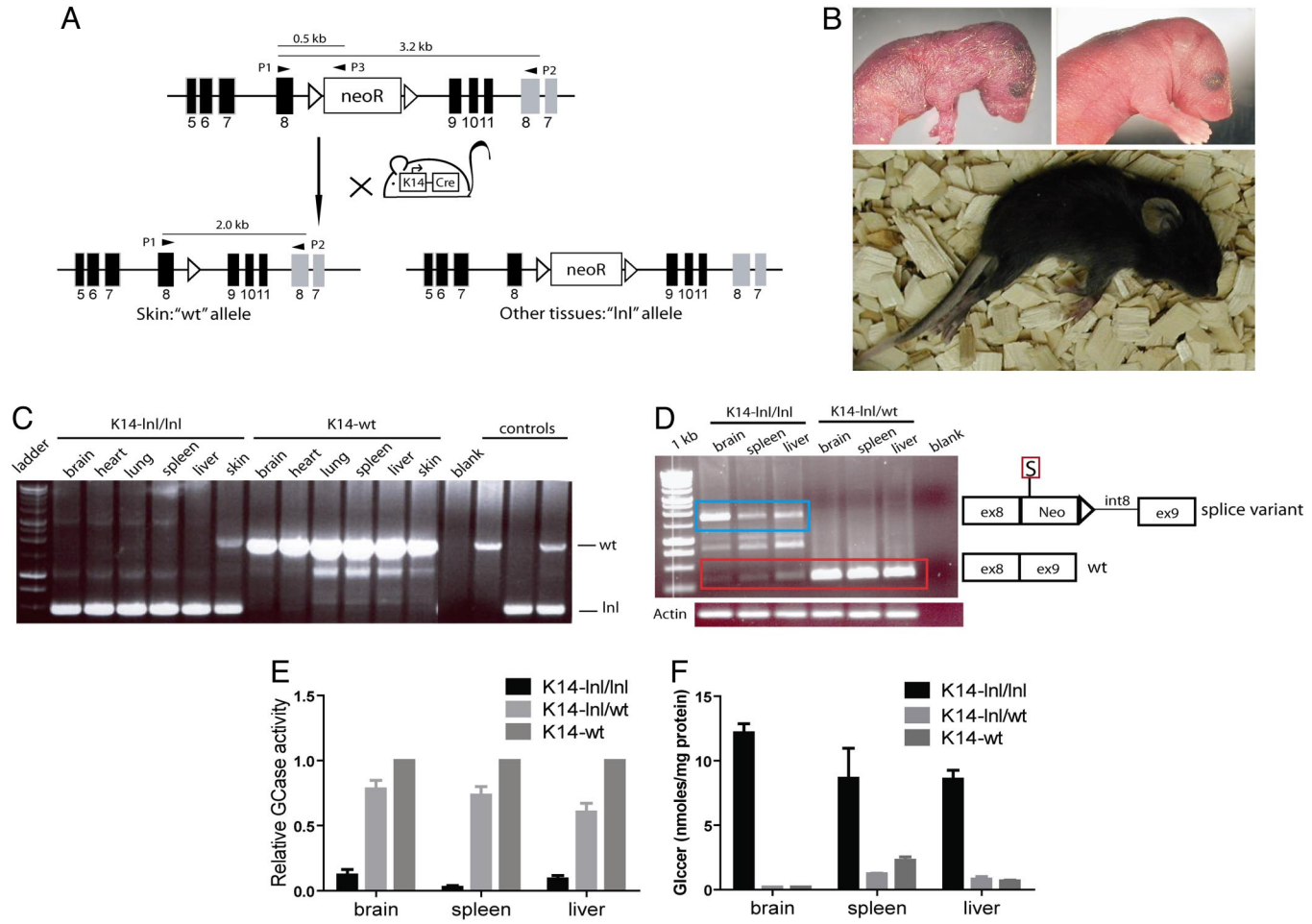

Fig. 1. Aberrant splicing of gba mRNA causes GCase deficiency in K14-Inl/Inl mice. (*A*) Schematic view of the generation of the K14-Inl/Inl mice; mice harbouring the Inl allele in intron 8 of the gba gene were bred with K14-Cre mice (21). K14-mediated expression of Cre enabled removal of the Inl cassette in the epidermis of the K14-Inl/Inl mice. Black bars represent gba exons, gray bars represent metaxin exons, open triangles represent loxP sites, and P1, P2, and P3 denote primer locations. (*B*) (*Upper Left*) The lethal skin phenotype in the newborn gba$^{Inl/Inl}$ mouse was similar to the phenotype of previous GCase-deficient mice (17, 19, 23). (*Upper Right*) Newborn littermate control [representative of both gba$^{Inl/+}$; K14-Cre (termed K14-Inl/wt) and gba$^{+/+}$; K14-Cre (termed K14-wt)]. (*Lower*) K14-Inl/Inl mouse at end stage (constant paralysis, ≈2 weeks old). (*C*) Representative PCR showing removal of the Inl cassette [visualized as presence of a wild-type (wt) band] in the skin of K14-Inl/Inl mice. (*D*) Retention of the Inl cassette in intron 8 of the gba gene causes aberrant splicing. (*Left*) A prominent splice-variant (blue box) was obtained through RT-PCR on brain, spleen, and liver specimens from K14-Inl/Inl mice. (*Right*) Schematic representation of the variant sequence. Correctly spliced gba mRNA was also present in these mice (red box). Actin was used as loading control. S, stop codon; ex, exon; int, intron; Neo, neomycin resistance gene. (*E*) GCase activity was severely reduced in brain, spleen, and liver of the K14-Inl/Inl mice (n = 4–7) compared with both K14-Inl/wt (n = 5–8) and K14-wt mice (n = 5). GCase activity in K14-wt mice was set to 1. All mice were 2 weeks old at the time of analysis. Error bars represent SD. (*F*) K14-Inl/Inl mice (n = 7) had elevated levels of Glccer in brain, spleen, and liver compared with K14-Inl/wt (n = 3) and K14-wt (n = 3) mice. Error bars represent SD.

viable, but with pathology restricted to the visceral tissues (17, 19, 20, 23), the K14-Inl/Inl mice developed a rapidly progressing neurological disease after an initial symptom-free period of ≈10 days. The K14-Inl/Inl mice showed symptoms of motor dysfunction including abnormal gait, hyperextension of the neck, and seizures (SI Movie 1), which are also common signs of acute neuronopathic GD (8, 9). The mice developed continuous seizures and were killed at 2 weeks of age, at end-stage paralysis (Fig. 1*B*).

K14-Inl/Inl mice had smaller brains than control animals (data not shown). All brain regions were present and had normal gross anatomy (Fig. 2 *A–H*), indicating that GCase does not have a fundamental role in the formation of the brain. Microscopic analysis, however, revealed a substantial reduction in cellular density throughout the brain, with some regions such as the cortex and thalamus being particularly affected (Fig. 2 *F–H*). The most prominently involved cortical layer (layer V) showed a profound loss of large pyramidal neurons (Fig. 2*G*), as reported in patients with type 2 GD (11, 12, 15). The cerebellum and nuclei of the pons and medulla also displayed a considerable reduction in the number of cells (SI Fig. 7). The reduction in cellular density was associated with abundant pyknotic nuclei (Fig. 2*I*). Large neurons were frequently surrounded by ameboid-shaped cells, which had the typical morphology of phagocytic microglia cells (Fig. 2*J*). Some neurons, especially in the motor trigeminal nuclei and pons region, had huge vacuoles within their cell bodies, suggesting neuronal accumulation of lipids because of GCase deficiency (Fig. 2 *K* and *L*). Similar neuronal vacuoles have been observed in patients (11). A marked increase in apoptotic cell death was observed in various regions of the brain, for example, in the thalamus, the dendate gyrus of the hippocampus, and the cerebellum in GCase-deficient mice compared with control animals as measured by TUNEL and activated caspase 3 (Fig. 3 *A–L*). We also observed increased labeling for TUNEL and activated caspase 3 in medulla and pons region (data not shown). Moreover, strong

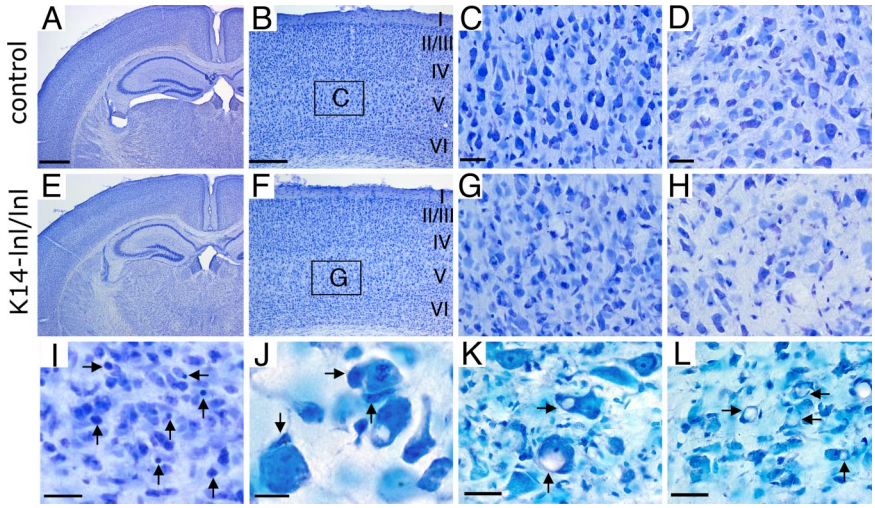

Fig. 2. Cell loss in brains of GCase deficient mice. Histological analyses of K14-Inl/wt (control) mice (*A–D*) and K14-Inl/Inl mice (*E–L*). Nissl staining of cryosections of brains from K14-Inl/Inl mice displayed normal brain architecture (*E*) similar to the control mice (*A*). Extensive loss of neurons was observed in the cortex (*F*) and thalamus (*H*). *C* and *G* are higher magnifications of the cortical layer V (indicated by squares labeled ''C'' and ''G'') from *B* and *F*, respectively. Note the loss of large pyramidal neurons in cortical layer V (*G*). (*H*) The thalamic region of mutant mice also showed a severe loss of neurons. (*I*) A large number of pyknotic cells (arrows) were scattered throughout the brain. (*J*) Neurons surrounded by microglia processes of one or several phagocytic cells with ameboid shapes (arrows) were frequently detected in regions with abundant apoptotic cell death. Note the presence of huge vacuoles (arrows) inside large neurons of the motor trigeminal nucleus (*K*) and pons region (*L*) of mutant mice. All K14-Inl/Inl mice and controls were ≈2 weeks old at analysis. In *B* and *F*, I–VI indicate the cortical layers. (Scale bars: *A*, 600 μm; *B*, 200 μm; *C*, *D*, *K*, and *L*, 30 μm; *I*, 20 μm; *J*, 10 μm. Scale of *E* matches *A*, *F* matches *B*, *G* matches *C*, and *H* matches *D*.)

FluoroJade B labeling of pyramidal neurons was selectively detected in cortical layer V of the K14-Inl/Inl brain, which further demonstrated neurodegeneration and indicated a differential vulnerability in neurons to the toxicity of the deficiency of GCase (Fig. 3*N*). Similarly, neurons of CA3 and dendate gyrus regions underwent degeneration in the hippocampus of animals with

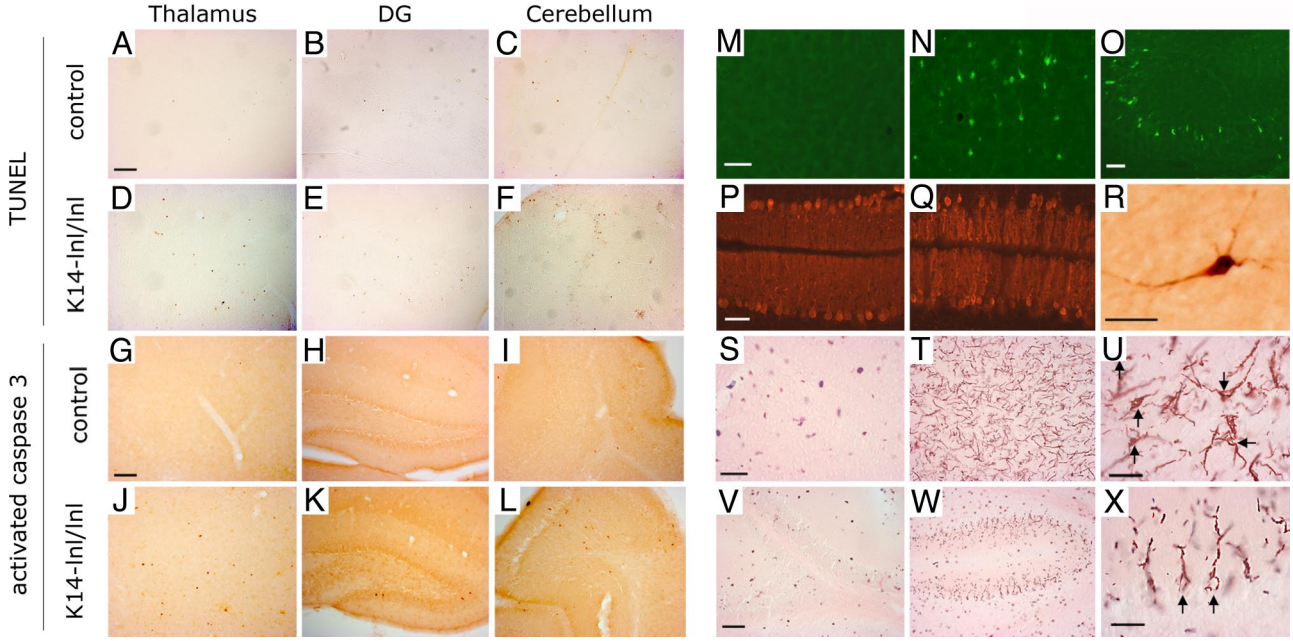

Fig. 3. Neuropathology and increased apoptotic cell death in GCase-deficient mice. Histological stainings for TUNEL (*A–F*) and activated caspase 3 (*G–L*). Compared with control mice (*A–C* and *G–I*), apoptotic cell death was abundantly increased in thalamus (*D* and *J*), dendate gyrus (DG) (*E* and *K*), and cerebellum (*F* and *L*) in K14-Inl/Inl mice. (*M–O*) FluoroJade B labeling was observed in K14-Inl/Inl mice (*N* and *O*) but not in control animals (*M*). Degenerating neurons were scattered throughout the brain in GCase-deficient mice as shown for the cortex (*N*) and hippocampus (*O*). (*P* and *Q*) In contrast to controls (*P*), calbindin-labeled Purkinje neurons were reduced in number and exhibited swollen dendrites in the mutant mice (*Q*). (*R*) The presence of activated caspase 3-positive cells with typical neuronal morphologies indicates apoptotic neuron death in K14-Inl/Inl mice. (*S-X*) Oil red O staining was used to detect lipid accumulation in control (*S* and *V*) and mutant (*T*, *U*, *W*, and *X*) mice. Regions in the medulla (*S–U*) and the cerebellum (*V–X*) displayed a marked accumulation of lipids in mutant animals. *U* and *X* are higher magnifications of *T* and *W*, respectively, and reveal the presence of lipids in both axons and cell bodies (arrows indicate neuronal cell bodies). Note the selective accumulation of lipids in both the cell bodies (arrows) and dendrites of Purkinje cells in the cerebellum of GCase deficient mice (*W* and *X*). Only background staining with nonspecific oil red O precipitates was observed in control brain sections (*S* and *V*). All K14-Inl/Inl mice and controls were ≈2 weeks old at analysis. [Scale bars: *A* (applies to *A–L*, *V*, and *W*), 100 μm; *M* (applies to *M–Q*, *S*, and *T*), 60 μm; *R*, *U*, and *X*, 30 μm.]

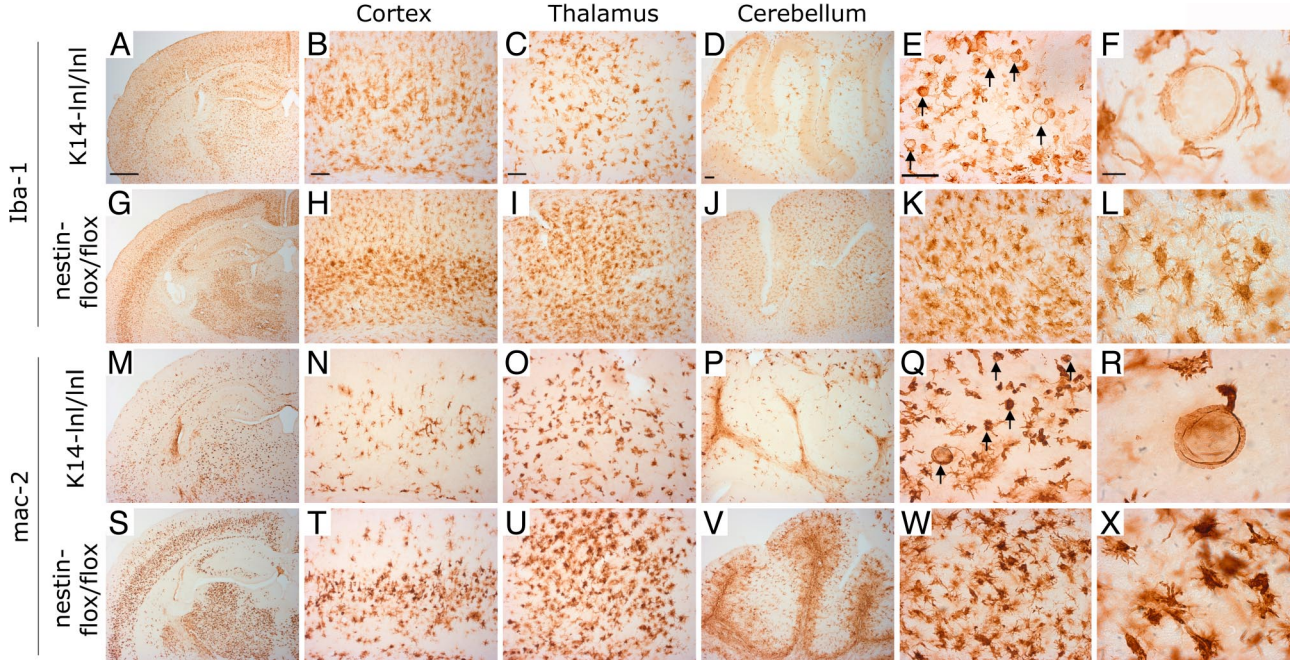

Fig. 4. Normal microglial function in the brain of Nestin-flox/flox mice. Immunostaining with microglia markers: Iba-1 (*A–L*) and mac-2 (*M–X*) in indicated brain regions of K14-lnl/lnl (*A–F* and *M–R*) and Nestin-flox/flox (*G–L* and *S–X*) mice. Iba-1 stains both resting and activated microglia, whereas mac-2 is more selective for activated/proliferating microglia (41–43). No mac-2 staining was observed in control animals. Higher magnification of the thalamic region shows the presence of lipid-engorged microglia (arrows) in K14-lnl/lnl mice (*E*, *F*, *Q*, and *R*) but not in Nestin-flox/flox mice (*K*, *L*, *W*, and *X*). Note the higher activation of microglia in Nestin-flox/flox animals (*G–L* and *S–X*) compared with K14-lnl/lnl mice (*A–F* and *M–R*), suggesting a proliferation defect of microglia in K14-lnl/lnl mice. All K14-lnl/lnl mice and Nestin-flox/flox mice were analyzed at end-stage paralysis, corresponding to an age of ≈2 and ≈3 weeks, respectively. (Scale bars: *A*, 600 μm; *B–E*, 80 μm; *F*, 20 μm. Scale within columns is uniform.)

reduced GCase activity (Fig. 3*O*), whereas the CA1 region was unaffected, again reflecting findings in type 2 GD patients (15). The calbindin marker for Purkinje neurons revealed a partial loss of these cells in the cerebellum and a profound swelling of their axons (Fig. 3 *P* and *Q*). The presence of activated caspase 3-stained cells with a typical neuronal morphology further confirmed the degeneration of neurons in the mutant mice (Fig. 3*R*). Oil red O staining revealed a substantial accumulation of lipid in both neuronal cell bodies and axons of the K14-lnl/lnl brains (Fig. 3 *T*, *U*, *W*, and *X*). We also observed a selective accumulation of lipid in the Purkinje cells of the cerebellum (Fig. 3 *W* and *X*). In contrast, control mice did not display specific oil red O staining (Fig. 3 *S* and *V*). In addition, massive astrogliosis and microglial proliferation, visualized by GFAP and Iba-1 immunostaining, respectively, were present in regions with the most pronounced neuronal loss (SI Fig. 8). These findings demonstrate that the K14-lnl/lnl mice exhibit severe neurodegenerative pathology similar to patients with acute neuronopathic GD (2, 10–16).

Mice with Neuronal and Macroglial GCase Deficiency, but Normal Microglial GCase Activity, Develop Signs Similar to K14-lnl/lnl Mice, but with Slower Progression. It is not known whether the severe neurodegenerative phenotype of type 2 GD is caused by GCase deficiency in neuronal cells, or whether GCase-deficient microglia/macrophages that are of hematopoietic origin (24, 25) play an important role in the pathogenesis of this condition. To restrict GCase deficieny to the progeny of neural and glial cell precursors while maintaining normal enzyme activity within microglial cells, we crossed Nestin-Cre (26) mice into $gba^{flox/flox}$ mice, creating $gba^{flox/flox}$; Nestin-Cre mice (referred to as Nestin-flox/flox throughout the text; SI Fig. 9). The Nestin-flox/flox mice were indistinguishable from littermates at birth but eventually developed signs similar to the K14-lnl/lnl mice. The onset of these signs was delayed in Nestin-flox/flox mice compared with K14-lnl/lnl mice (2–3 weeks vs. 10 days, respectively). The neurological abnormalities included rigidity of limbs and abnormal gait, which eventually led to constant seizures and paralysis (defined as end stage) on average 1 week later in the Nestin-flox/flox mice than the K14-lnl/lnl mice (SI Fig. 9). The progression from onset of symptoms to end-stage paralysis was slower in the Nestin-flox/flox mice compared with the K14-lnl/lnl mice (7–10 days vs. 3–4 days, respectively), suggesting that although GCase deficiency within microglia is not the primary contributor to the neurodegeneration in our mouse models, they might influence the onset and progression of the disease. At end-stage paralysis, the Nestin-flox/flox mice demonstrated a severe reduction in GCase activity in the brain compared with spleen, liver, and $gba^{+/+}$; Nestin-Cre mice (hereafter referred to as Nestin-wt) (SI Fig. 9). Increased Glccer was observed in brain tissue of Nestin-flox/flox mice but not in tissues from control mice (Nestin-wt and Nestin-lnl/wt) (SI Fig. 9).

GCase Activity Is Critical for Neuronal Survival. Similar to K14-lnl/lnl, Nestin-flox/flox mice developed massive neuronal loss, astrogliosis (data not shown), and microgliosis (Fig. 4). The most striking difference between these mutant mice appeared at the level of microglial activation (Fig. 4). By using microglial markers Iba-1 and mac-2, substantial changes in size, number, and morphology of microglia cells was clearly evident in various brain regions such as cortex, thalamus, and cerebellum in both K14-lnl/lnl and Nestin-flox/flox mice (Fig. 4). Because the nestin promoter is active in neuronal and glial progenitors and microglia are of hematopoietic origin (24, 25), microglial cells in Nestin-flox/flox mice were expected to have normal GCase activity. GCase activity in hematopoietic cells from the Nestin-flox/flox mice was, indeed, normal (data not shown), strongly indicating normal GCase activity in microglial cells. Moreover,

higher levels of Glccer were present within the brains of K14-lnl/lnl mice compared with Nestin-flox/flox brains and, importantly, lipid-engorged microglia cells could only be found in K14-lnl/lnl animals (Figs. 1*F*, 4 *F* and *R*, and SI Fig. 9), further supporting normal GCase activity in microglial cells of the Nestin-flox/flox brain. As expected, we observed activation of microglia in brain regions associated with more-severe cell death in both K14-lnl/lnl and Nestin-flox/flox mice. Interestingly, Nestin-flox/flox mice exhibited a more profound activation and proliferation of microglial cells than K14-lnl/lnl mice (Fig. 4), suggesting that GCase deficiency within microglial cells decreased the level of microglia proliferation and/or activation in response to the considerable cell death. Together, these results show that GCase activity is critical for neuronal survival and indicate that loss or reduction of GCase activity in microglia is likely responsible for the more-rapid progression of neuropathology in K14-lnl/lnl mice compared with Nestin-flox/flox mice.

Discussion

In this study, we describe the development of two mouse models of the severe neuronopathic form of GD. The disease phenotype in the K14-lnl/lnl mouse, in which the GCase deficiency is caused by abnormal splicing of the gba transcript, shows a close resemblance to patients with type 2 GD in terms of clinical signs and histopathological findings within the CNS. Similar to GD patients, we also found elevated quantities of the second substrate for GCase; glucosylspingosine in the brain of the K14-lnl/lnl mice (data not shown). Previous studies have revealed that accumulation of glucosylsphingosine results in neuronal toxicity (27, 28). Our mouse models have implications in the investigation of pathogenic mechanisms that are involved in the CNS manifestations of type 2 GD.

A frequent finding in the brains of patients with type 2 GD is activation and proliferation of microglia (10–13, 29). We observed massive activation of microglia in various regions in the brain of the K14-lnl/lnl mice. We found several swollen microglia that were almost 100 times the size of normal resting microglia (Fig. 4). Although it has been anticipated that GCase-deficient neurons are responsible for the severe CNS symptoms, this has never been verified. We therefore wished to learn if the massive storage and/or subsequent activation of microglia were responsible for the severe neurological abnormalities in the K14-lnl/lnl mice, because activation of microglia cells has been shown to be involved in other neurodegenerative disorders (30–33). The Nestin-Cre mice have previously been widely applied to create conditional deletion of genes within the CNS and have been shown to induce efficient and widespread recombination in precursors of both neurons and glia, such as astrocytes and oligodendrocytes (26, 34–36). The CNS-restricted GCase deficiency in the Nestin-flox/flox mouse caused a disease phenotype that was similar to the K14-lnl/lnl mouse, although the onset of manifestations was delayed and progression of the disease was slower. Indeed, microglia have recently been reported to affect disease progression in mouse models of neurodegenerative disorders such as amyotrophic lateral sclerosis (32). There was a higher degree of activation and proliferation of microglia within the Nestin-flox/flox brain compared with the K14-lnl/lnl brain demonstrating that these hematopoietically derived cells are likely to function normally in the Nestin-flox/flox mice. We cannot, however, exclude the possibility that alterations of GCase activity in other nonneuronal cells may also contribute to the observed neurodegenerative phenotype. The results suggest that although GCase-deficient microglia cells are not primary determinants of the CNS pathogenesis in GCase deficient mice, they contribute by influencing the onset and progression of the disease. Our data suggest that restoration of GCase activity in cells of hematopoietic origin (including microglia) through conventional bone marrow transplantation might slow disease progression but is unlikely to cure GD patients with severe CNS involvement. It is possible that overexpression of GCase within hematopoietic stem cells after gene transfer may be more effective than transplantation of unmodified cells, but this needs to be thoroughly tested. It is not clear whether gene therapy of a proportion of the cells in the CNS will result in a clinical benefit. Selection of an appropriate GCase vector, delivery method, and target cells will require careful consideration to achieve total correction of the disease.

In conclusion, our mouse model (K14-lnl/lnl) shows high similarity, both in pathological findings and clinical manifestations, to patients with severe neuronopathic GD. Our study also indicates that GCase deficiency in microglial cells is not the primary determinant in the CNS pathogenesis of GD but may influence disease onset and progression. It is anticipated that both of the models generated in this study will be valuable in investigations on the pathogenesis as well as in the development of therapy for patients with neuronopathic GD.

Materials and Methods

Generation of Transgenic Mice. A detailed description of the generation of the mice in this study and genotype screening through PCR is available in *SI Materials and Methods*. K14-Cre mice (21) were interbred to generate $gba^{lnl/lnl}$; K14-Cre mice (referred to as K14-lnl/lnl throughout the text). Control animals $gba^{lnl/+}$; K14-Cre and $gba^{+/+}$; K14-Cre are referred to as K14-lnl/wt and K14-wt, respectively. $Gba^{flox/flox}$ mice (20) were crossed with Nestin-Cre mice (26) (a kind gift from Klas Kullander, Uppsala University, Uppsala, Sweden) to generate $gba^{flox/flox}$; Nestin-Cre mice (referred to as Nestin-flox/flox throughout the text). Control animals consisted of $gba^{flox/+}$; Nestin-Cre (referred to as Nestin-flox/wt) and $gba^{+/+}$; Nestin-Cre (referred to as Nestin-wt).

Histochemical Analysis. Information on tissue preparatory procedures is available in *SI Materials and Methods*. The following primary antibodies were used: rabbit Ab anti-GFAP (1:1,000; Dako, Glostrup, Denmark), rabbit Ab anti-Iba-1 (1:1,000; Wako, Osaka, Japan), rabbit Ab anti-calbindin D-28 (1:500; Swant, Bellinzona, Switzerland), rabbit anti-cleaved caspase 3 (1:100; Cell Signaling Technology, Beverly, MA), and rat Ab anti-mac-2 (1:500; Cedarlane, Ontario, Canada). Apoptotic cells were also detected with TUNEL assay by using ApopTag peroxidase *in situ* kit (Chemicon, Temecula, CA). FluoroJade B (Chemicon) and Nissl stainings were performed as described previously (37). Lipid accumulations in brain slices were revealed with 0.5% oil red O (Sigma, Stockholm, Sweden) in 60% isopropanol.

RT-PCR, cDNA Sequencing, and Q-RT-PCR. A detailed description of RT-PCR and sequencing procedures are available in *SI Materials and Methods*.

Substrate Accumulation Analysis and Histopathological Studies. Information concerning these procedures is available in *SI Materials and Methods*. The glucosylceramide content was determined as previously described (38). Fixed, sectioned tissue was stained with hematoxylin-eosin or periodic acid/Schiff (PAS) for microscopic examination.

Enzyme Assay. Cells were lysed by three freeze/thaw cycles. Aliquots of the lysate where incubated for 40 min at 37°C with or without 400 μM Conduritol B Epoxide (39) (CBE; Sigma–Aldrich, St. Louis, MO). GCase activities were determined fluorimetrically after 2 h incubation at 37°C with 15 mM 4-MUG (Sigma–Aldrich) (40). In all assays, control cells were analyzed, and the level in these was set to 1.

We thank Lottie Jansson-Sjöstrand, Jonas Larsson, Per Levéen, Britt-Marie Rynmark, and Eva Gynnstam for both technical assistance and valuable discussions throughout this study; Jens Bohne for his expert knowledge and advice during the investigation of the splicing defect in the K14-lnl/lnl mouse; and Professor Anders Björklund for fruitful discussions. C.L.B. was supported by the Michael J. Fox foundation, European Molecular Biology Organization, Swedish Parkinson Foundation, and the Swiss National Science Foundation. S.K. was supported by the Swedish Cancer Society, the European Commission [Gene Therapy for Hereditary Diseases (INHERINET) and Concerted Safety and Evaluation of Retroviral Transgenesis in Gene Therapy of Inherited Diseases (CONSERT)], the Swedish Gene Therapy Program, the Swedish Children's Cancer Foundation, a Clinical Research Award from Lund University Hospital, the Joint Program on Stem Cell Research (supported by the Juvenile Diabetes Research Foundation), and the Swedish Medical Research Council. The Lund Stem Cell Center is supported by a Center of Excellence grant in life sciences from the Swedish Foundation for Strategic Research.

1. Brady RO, Kanfer JN, Bradley RM, Shapiro D (1966) *J Clin Invest* 45:1112–1115.
2. Beutler E, Grabowski GA (2001) in *The Metabolic and Molecular Bases of Inherited Disease*, eds Scriver CR, Beaudet AL, Sly WS, Valle D (McGraw–Hill, New York), pp 3635–3668.
3. Barton NW, Furbish FS, Murray GJ, Garfield M, Brady RO (1990) *Proc Natl Acad Sci USA* 87:1913–1916.
4. Barton NW, Brady RO, Dambrosia JM, Di Bisceglie AM, Doppelt SH, Hill SC, Mankin HJ, Murray GJ, Parker RI, Argoff CE, *et al.* (1991) *N Engl J Med* 324:1464–1470.
5. Figueroa ML, Rosenbloom BE, Kay AC, Garver P, Thurston DW, Koziol JA, Gelbart T, Beutler E (1992) *N Engl J Med* 327:1632–1636.
6. Grabowski GA, Barton NW, Pastores G, Dambrosia JM, Banerjee TK, McKee MA, Parker C, Schiffmann R, Hill SC, Brady RO (1995) *Ann Intern Med* 122:33–39.
7. Prows CA, Sanchez N, Daugherty C, Grabowski GA (1997) *Am J Med Genet* 71:16–21.
8. Mignot C, Doummar D, Maire I, De Villemeur TB (2006) *Brain Dev* 28:39–48.
9. Tayebi N, Reissner KJ, Lau EK, Stubblefield BK, Klineburgess AC, Martin BM, Sidransky E (1998) *Pediatr Res* 43:571–578.
10. Lloyd OC, Norman RM, Urich H (1956) *J Pathol Bacteriol* 72:121–131.
11. Adachi M, Wallace BJ, Schneck L, Volk BW (1967) *Arch Pathol* 83:513–526.
12. Espinas OE, Faris AA (1969) *Neurology* 19:133–140.
13. Kaye EM, Ullman MD, Wilson ER, Barranger JA (1986) *Ann Neurol* 20:223–230.
14. Cervos-Navarro J, Zimmer C (1990) *Clin Neuropathol* 9:310–313.
15. Wong K, Sidransky E, Verma A, Mixon T, Sandberg GD, Wakefield LK, Morrison A, Lwin A, Colegial C, Allman JM, *et al.* (2004) *Mol Genet Metab* 82:192–207.
16. Wong K (2007) in *Gaucher Disease*, eds Futerman A, Zimran A (Taylor & Francis, Boca Raton, FL), pp 225–248.
17. Tybulewicz VL, Tremblay ML, LaMarca ME, Willemsen R, Stubblefield BK, Winfield S, Zablocka B, Sidransky E, Martin BM, Huang SP (1992) *Nature* 357:407–410.
18. Holleran WM, Ginns EI, Menon GK, Grundmann JU, Fartasch M, McKinney CE, Elias PM, Sidransky E (1994) *J Clin Invest* 93:1756–1764.
19. Xu YH, Quinn B, Witte D, Grabowski GA (2003) *Am J Pathol* 163:2093–2101.
20. Enquist IB, Nilsson E, Ooka A, Mansson JE, Olsson K, Ehinger M, Brady RO, Richter J, Karlsson S (2006) *Proc Natl Acad Sci USA* 103:13819–13824.
21. Jonkers J, Meuwissen R, van der Gulden H, Peterse H, van der Valk M, Berns A (2001) *Nat Genet* 29:418–425.
22. Nilsson O, Svennerholm L (1982) *J Neurochem* 39:709–718.
23. Liu Y, Suzuki K, Reed JD, Grinberg A, Westphal H, Hoffmann A, Doring T, Sandhoff K, Proia RL (1998) *Proc Natl Acad Sci USA* 95:2503–2508.
24. Hess DC, Abe T, Hill WD, Studdard AM, Carothers J, Masuya M, Fleming PA, Drake CJ, Ogawa M (2004) *Exp Neurol* 186:134–144.
25. Chan WY, Kohsaka S, Rezaie P (2007) *Brain Res Rev* 53:344–354.
26. Tronche F, Kellendonk C, Kretz O, Gass P, Anlag K, Orban PC, Bock R, Klein R, Schutz G (1999) *Nat Genet* 23:99–103.
27. Orvisky E, Sidransky E, McKinney CE, Lamarca ME, Samimi R, Krasnewich D, Martin BM, Ginns EI (2000) *Pediatr Res* 48:233–237.
28. Schueler UH, Kolter T, Kaneski CR, Blusztajn JK, Herkenham M, Sandhoff K, Brady RO (2003) *Neurobiol Dis* 14:595–601.
29. Mignot C, Gelot A, Bessieres B, Daffos F, Voyer M, Menez F, Fallet Bianco C, Odent S, Le Duff D, Loget P, *et al.* (2003) *Am J Med Genet A* 120:338–344.
30. Gonzalez-Scarano F, Baltuch G (1999) *Annu Rev Neurosci* 22:219–240.
31. Borchelt DR (2006) *N Engl J Med* 355:1611–1613.
32. Boillee S, Yamanaka K, Lobsiger CS, Copeland NG, Jenkins NA, Kassiotis G, Kollias G, Cleveland DW (2006) *Science* 312:1389–1392.
33. Monk PN, Shaw PJ (2006) *Nat Med* 12:885–887.
34. Gao Q, Wolfgang MJ, Neschen S, Morino K, Horvath TL, Shulman GI, Fu XY (2004) *Proc Natl Acad Sci USA* 101:4661–4666.
35. Jiang Y, de Bruin A, Caldas H, Fangusaro J, Hayes J, Conway EM, Robinson ML, Altura RA (2005) *J Neurosci* 25:6962–6970.
36. Graus-Porta D, Blaess S, Senften M, Littlewood-Evans A, Damsky C, Huang Z, Orban P, Klein R, Schittny JC, Muller U (2001) *Neuron* 31:367–379.
37. Lo Bianco C, Ridet JL, Schneider BL, Deglon N, Aebischer P (2002) *Proc Natl Acad Sci USA* 99:10813–10818.
38. Kyllerman M, Conradi N, Mansson JE, Percy AK, Svennerholm L (1990) *Acta Paediatr Scand* 79:448–453.
39. Grabowski GA, Osiecki-Newman K, Dinur T, Fabbro D, Legler G, Gatt S, Desnick RJ (1986) *J Biol Chem* 261:8263–8269.
40. Fink JK, Correll PH, Perry LK, Brady RO, Karlsson S (1990) *Proc Natl Acad Sci USA* 87:2334–2338.
41. Dong S, Hughes RC (1997) *Glycoconj J* 14:267–274.
42. Kriz J, Nguyen MD, Julien JP (2002) *Neurobiol Dis* 10:268–278.
43. Kriz J, Gowing G, Julien JP (2003) *Ann Neurol* 53:429–436.